# Involvement of conserved asparagine and arginine residues from the N-terminal region in the catalytic mechanism of rat liver and *Trypanosoma cruzi* tyrosine aminotransferases

VERÓNICA R. SOBRADO,[1] MARISA MONTEMARTINI-KALISZ,[2,3] HENRYK M. KALISZ,[2,3] MARÍA CANDELARIA DE LA FUENTE,[1] HANS-JÜRGEN HECHT,[2] AND CRISTINA NOWICKI[1]

[1]IQUIFIB (CONICET, Facultad de Farmacia y Bioquímica, Universidad de Buenos Aires), Buenos Aires, Argentina
[2]GBF, Gesellschaft für Biotechnologische Forschung, Braunschweig, Germany

(RECEIVED August 28, 2002; FINAL REVISION February 17, 2003; ACCEPTED February 19, 2003)

**Abstract**

Rat liver and *Trypanosoma cruzi* tyrosine aminotransferases (TATs) share over 40% sequence identity, but differ in their substrate specificities. To explore the molecular features related to these differences, comparative mutagenesis studies were conducted on full length *T. cruzi* TAT and N-terminally truncated rat TAT recombinant enzymes. The functionality of Arg315 and Arg417 in rat TAT was investigated for comparison with the conserved Arg292 and Arg386 in aspartate and bacterial aromatic aminotransferases (ASATs and ARATs). The rat TAT Arg315Lys variant remained fully active indicating that, as in *T. cruzi* TAT and contrary to subfamily Iα aminotransferases, this residue is not critical for activity. In contrast, the Arg417Gln variant was inactive. The catalytic relevance of the putative rat TAT active site residues Asn54 and Arg57, which are strictly conserved in TATs (Asn17 and Arg20 in *T. cruzi* TAT) but differ in ASATs and ARATs, was also explored. The substitutions Arg57Ala and Arg57Gln abolished enzymatic activity of these mutants. In both variants, spectral studies demonstrated that aromatic but not dicarboxylic substrates could efficiently bind in the active site. Thus, Arg57 appears to be functionally equivalent to Arg292 of ASATs and ARATs. Asn54 also appears to be involved in the catalytic mechanism of rat TAT since its exchange for Ser lowered the $k_{cat}/K_m$ ratios towards its substrates. Mutation of the analogous residues in *T. cruzi* TAT also lowered the catalytic efficiencies ($k_{cat}/K_m$) of the variants substantially. The results imply that the mamalian TAT is more closely related to the *T. cruzi* TAT than to ASATs and ARATs.

**Keywords:** Aromatic aminotransferases; rat liver tyrosine aminotransferase; heterologous expression; site directed mutagenesis; *Trypanosoma cruzi*

Aminotransferases belong to the α-family of vitamin $B_6$-dependent enzymes (Alexander et al. 1994), which play important roles in amino acid biosynthesis and degradation and carbohydrate metabolism in both prokaryotes and eukaryotes. These enzymes possess varied substrate specificities that mainly involve the three 2-oxoacids generated during glycolytic and respiratory cycles. Based on extensive structural, kinetic and site-directed mutagenesis studies on aspartate aminotransferases (ASATs), a ping-pong Bi-Bi mechanism involving several intermediates was proposed for the reversible transamination reaction. Furthermore, the substrate recognition mechanism of ASATs is the best understood among aminotransferases (Kirsch et al. 1984; Arnone et al. 1985; Hayashi 1995).

At the structural level, two different aminotransferases belonging to subfamily Iα, the highly specific mammalian

Reprint requests to: Cristina Nowicki, IQUIFIB (CONICET, Facultad de Farmacia y Bioquímica, Universidad de Buenos Aires), Junín 956, CP 1113 Buenos Aires, Argentina; e-mail: cnowicki@criba.edu.ar; fax: 54-114-962-5457.

[3]Present address: Biology Department, Pharmacia Italia SpA, I-20014 Nerviano, Italy.

Article and publication are at http://www.proteinscience.org/cgi/doi/10.1110/ps.0229403.

ASATs and the less specific bacterial aromatic aminotransferases (ARATs), are the most extensively investigated (Ford et al. 1980; McPhalen et al. 1992; Malashkevich et al. 1995a; Okamoto et al. 1998). In both enzymes, two arginine residues (Arg386 and Arg292, numbering corresponds to the cytosolic pig ASAT) were shown to be responsible for substrate specificity (Kirsch et al. 1984; Hayashi et al. 1996; Okamoto et al. 1998). The guanidine group of Arg386 interacts with the Cα-carboxylate group of the substrate. Arg292 plays a dual function in the active site. In all known Iα aminotransferases it forms a hydrogen bond with the β-carboxylate group of the dicarboxylic substrates; in the less specific ARATs it also forms nonpolar interactions through its side chain with aromatic substrates (Malashkevich et al. 1995b; Oue et al. 1997). In contrast, the subtle catalytic process involved in substrate recognition of aminotransferases that use nondicarboxylic substrates, such as tyrosine, methionine, or alanine, is still not clearly understood.

One of the most studied aromatic aminotransferases not belonging to subfamily Iα is tyrosine aminotransferase (TAT) from the primitive eukaryote *Trypanosoma cruzi*, the causative agent of American Trypanosomiasis. This enzyme has a very broad substrate specificity, efficiently utilizing leucine, methionine, tyrosine, phenylalanine, tryptophan, and alanine as amino donors (Montemartini et al. 1993; Nowicki et al. 2001). Crystallographic, kinetic and mutagenesis studies on *T. cruzi* TAT demonstrated that Arg389, which corresponds to the strictly conserved Arg386 in ASATs, is essential for substrate binding. In contrast, Arg283, which is situated in the region of Arg292 of ASATs, plays no role in catalysis (Blankenfeldt et al. 1999; Nowicki et al. 2001). *T. cruzi* TAT, which belongs to the aminotransferase family I but to date has not been definitively assigned to any of its subfamilies, shares a sequence identity of nearly 40% (70% similarity) with the mammalian liver TATs, classified by Jensen and Gu (1996) as belonging to subfamily Iγ. Mammalian liver TATs are hormonally inducible enzymes with a short intracellular half-life ($t_{1/2}$ = 2 h) and a high specificity for the tyrosine/2-oxoglutarate substrate pair (Iwasaki et al. 1973). Their molecular mass (50 kD) is higher than that of the ASATs (43 kD) or *T. cruzi* TAT (45 kD). Sequence alignments show a low degree of identity (~25%) between mammalian TATs and vertebrate and prokaryotic ASATs. In addition, the mammalian enzymes possess extensions in their N- and C-termini (Fig. 1). Mammalian TATs have been considered for a long time as attractive models for the understanding of the hormonal regulation of transcription in eukaryotes. However, the low yields, instability, and heterogeneity of the liver enzyme have hampered structure–function relationship studies on these enzymes. Although Dietrich et al. (1991) established high level expression conditions for rat TAT in prokaryotic cells, at least five different purification steps were required to obtain enzyme homogeneity, and detailed structural characterization studies have not been performed to date. Hence, no information is available about the functional roles of active site residues of mammalian TATs.

Herein we report the functional expression in bacteria of an N-terminally truncated and His-tagged rat liver TAT and its purification by one-step affinity chromatography. Comparative studies show that in rat TAT, Arg315, which is conserved in mammalian TATs in the region of Arg292 in ASATs and ARATs, according to the structure-based sequence alignment, is not involved in catalysis. On the contrary, Asn54 and Arg57 (equivalent to Asn17 and Arg20 in *T. cruzi* TAT) showed to be essential for the catalytic process in both enzymes. Furthermore, Arg417 of rat TAT, a strictly conserved residue in all known aminotransferases, seems to be essential for enzymatic activity, resembling the functionality of Arg386 in ASATs and ARATs and that of Arg389 in *T. cruzi* TAT.

## Results

### *Functional heterologous expression and purification of N-terminally truncated rat liver TAT*

Based on previous observations of Stellwagen (1992) and our structure-based sequence alignments (Blankenfeldt et al. 1999), recombinant rat TAT was expressed as an N-terminlly truncated form, being shortened by the first 37 amino acids compared to the naturally expressed form in liver cells (Fig. 1). A six-histidine Tag was attached to the N-terminus to simplify its purification. Induction of bacteria for 4 h, at 28°C, resulted in the accumulation of a new protein with an apparent molecular weight of 45 kD in SDS gels, that was recognized by the antirat TAT-specific antiserum (data not shown). A final yield of nearly 16 mg pure rat TAT per liter of bacterial culture was obtained by affinity chromatography on a $Ni^{2+}$ column. The average specific activity of the recombinant N-truncated rat TAT (340 $U \cdot mg^{-1}$) was identical to that previously reported for the full-length protein towards its highly specific substrates, tyrosine and 2-oxoglutarate (Dietrich et al. 1991).

### *Structural characterization of the recombinant rat TAT*

At least 10 different peptide fractions with an absorbance ratio 254/280 ≥ 1 were detected when recombinant rat TAT modified with 4-vinylpyridine under denaturing conditions and digested with trypsin was fractionated by reverse phase HPLC. The peptides containing at least one 4-ethylpyridylcysteine residue in their amino acid sequence are listed in

```
Tc-TAT      ------------------------------------MSSWDVSMSNHAGLV-FNPIRTVSDNAKPSP-SPKPI
Hum-TAT     MDPYMIQMSSKGNLPSILDVHVNVGGRSSVPGKMKGRKARWSVRPSDMAK-KTFNPIRAIVDNMKVKPNPNKTM
RatTAT      mdsyviqtdvddslssvldvhvniggrnsvqgrkkgrKARWDVRPSDMSN-KTFNPIRAIVDNMKVQPNPNKTV
Pd-ARAT     ------------------------------------MLGNLKP------QAPDKILALMGEFRADP-RQ-GK
Ecoli-ASAT  ------------------------------------MFENITA------APADPILGLADLFRADE--RPGK
Tb-mASAT    -------------------------------------------------MGKPDPILGLGQDFRMDP-AKR-K
Ecoli-ARAT  ------------------------------------MFQKVDAY------AGDPILTLMERFKEDP--RSDK

Tc-TAT      IKLSVGDPT-LDKNLLTSAAQIKKLKEAIDSQEC--NGYFPTVGSPEAREAVATWWRNSFVHKEELKSTIVKDN
Hum-TAT     ISLSIGDPTVFGNLPTDPE-VTQAMKDALDSGKY--NGYAPSIGFLSSREEIASYYHCP-------EAPLEAKD
Rat-TAT     ISLSIGDPTVFGNLPTDPE-VTQAMKDALDSGKY--NGYAPSIGYLSSREEVASYYHCH-------EAPLEAKD
Pd-ARAT     IDLGVGVYKDATGHTPIMRAVHAAEQRMLETET-T-KTYAGLSGEPEFQKAMGELILGD-GLK---SETTA---
Ecoli-ASAT  INLGIGVYKDETGKTPVLTSVKKAEQYLLENETTKN--YLGIDGIPEFGRCTQELLFGK----GSALINDKRAR
Tb-mASAT    VNLSIGVYRDDADQPFVLEC---VKQATLGTNMDY----APVTGIASFVEEAQKLCFGP----TCAALRDGRIA
Ecoli-ARAT  VNLSIGLYYNEDGIIPQLKAVAEAEARLNAVPHG-ASLYLPMEGLNSYRHAIAPLLFGADHP----VLQQQRVA

Tc-TAT      VVLCSGGSHGILMAITAICD---AGDYALVPQPGFPHYETVCKAYGIGMHFYN-CRPENDWEADLDEIRRL---
Hum-TAT     VILTSGCSQAIDLCLAVLAN---PGQNILVPRPGFSLYKTLAESMGIEVKLYN-LLPEKSWEIDLKQLEYLID-
Rat-TAT     VILTSGCSQAIELCLAVLAN---PGQNILIPRPGFSLYRTLAESMGIEVKLYN-LLPEKSWEIDLKQLESLID-
Pd-ARAT     TLATVGGTGALRQALELARMA-NPDLRVFVSDPTWPNHVSIMNFMGLPVQTYRYFDAETR-GVDFEGMKADLAA
Ecoli-ASAT  TAQTPGGTGALRVAADFLAKN-TSVKRVWVSNPSWPNHKSVFNSAGLEVREYAYYDAENH-TLDFDALINSLN-
Tb-mASATD   SCQTLGGTGALRIGGDLLNRFVANCNRIYGPDVGYPNHESIFAKAGMELTPYSYYDPATK-GFNLAGMLECLDQ
Ecoli-ARAT  TIQTLGGSGALKVGADFLKRYFP-ESGVWVSDPTWENHVAIFAGAGFEVSTYPWYDEATN-GVRFNDLLAMLK-

Tc-TAT      -KDDKTKLLIVTNP-SNPCGSNFSRKHVEDIVRLAEELRLPLFSDEIYAGMVFKGKDPNATFTSVADFETTVPR
Hum-TAT     ---EKTACLIVNNP-SNPCGSVFSKRHLQKILAVAARQCVPILADEIYGDMVFSDCK----YEPLATLSTDVPI
Rat-TAT     ---EKTACLVVNNP-SNPCGSVFSKRHLQKILAVAERQCVPILADEIYGDMVFSDCK----YEPLANLSTNVPI
Pd-ARAT     -AKKGD-MVLLHGCCHNPTGANLTLDQWAEIASILEKTGALPLIDLAYQGFGDGLEE-DAAGTRLIASRIP-EV
Ecoli-ASAT  -EAQAGDVVLFHGCCHNPTGIDPTLEQWQTLAQLSVEKGWLPLFDFAYQGFARGLEE-DAEGLRAFAAMHK-EL
Tb-mASAT    GRLRGSVKTRSMPAQHNPTGVDPTHDDWRQVCDVIKRRNHIPFVDMAYPSFATGQLDYDAFVPRHLVDMVP-NL
Ecoli-ARAT  -TLPARSIVLLHPCCHNPTGADLTNDQWDAVIEILKARELIPFLDIAYQGFGAGMEED-AYAIRAIASAGL-PA

Tc-TAT      VILGGTAKNLVVPGWRLGWLLYVDP-HGNGPSFLEGLKRVGML-VCGPCTVVQAALGEALLN-----TPQEHLD
Hum-TAT     LSCGGLAKRWLVPGWRLGWILIHDRRDIFGNEIRDGLVKLSQR-ILGPCTIVQGALKSILCR-----TPGEFYH
Rat-TAT     LSCGGLAKRWLVPGWRLGWILIHDRRDIFGNEIRDGLVKLSQR-ILGPCTIVQGALKSILQR-----TPQEFYH
Pd-ARAT     LIAASCSKNFGIYRERTGCLLALCADAATRELAQGAMAFLNRQTYSFPPFHGAKIVSTVLTTPELRADWMAELE
Ecoli-ASAT  IVASSYSKNFGLYNERVGACTLVAADSETVDRAFSQMKAAIRANYSNPPAHGASVVATILSNDALRAIWEQELT
Tb-mASAT    IVAQSFSKNFGLYGHRCGALHLSTASAEEAKRLVSQLALLIRPMYSNPPLYGAWVVSSILKDPQLTALWKKELK
Ecoli-ARAT  LVSNSFSKIFSLYGERVGGLSVLCEDAEAAGRVLGQLKATVRRNYSSPPNFGAQVVAAVLNDEALKASWLAEVE

Tc-TAT      QIVAKIEESAMYLYNHIGECIGLAPTMPRGAMYLMSRIDLEKYRDIKTDVEFFEKLLEEENVQVLPGTIFHAPG
Hum-TAT     NTLSFLKSNADLCYGALAAIPGLRPVRPSGAMYLMVGIEMEHFPEFENDVEFTERLVAEQSVHCLPATCFEYPN
Rat-TAT     DTLSFLKSNADLCYGALAAIPGLQPVRPSGAMYLMVGIEMEHFPEFENDVEFTERLIAEQAVHCLPATCFEYPN
Pd-ARAT     AVRSGMLRLREQLAGELRDLSG---SDRFGFVAEHRGMFSRLGATPEQVKRIKEEFGIYMVG------------
Ecoli-ASAT  DMRQRIQRMRQLFVNTLQEKGANR-DFSFIIKQNGMFSFSGLTKEQVLRLREEFGVYAVAS-------------
Tb-mASAT    QMSSRIAEVRKRLVSELKACGSVH-DWSHIERQVGMMAYTGLTREQVELLRSEYHIYMTLN-------------
Ecoli-ARAT  EMRTRILAMRQELVKVLSTEMPER-NFDYLLNQRGMFSYTGLSAAQVDRLREEFGVYLIAS-------------

Tc-TAT      FTRLTTT-RPVEVYREAVERIKAFCQRHAAV
Hum-TAT     FIRVVIT-VPEVMMLEACSRIQEFCEQHYHCAEGSQEECDK
Rat-TAT     FFRVVIT-VPEVMMLEACSRIQEFCEQHYHCAEGSQEECDK
Pd-TAT      DSRINIAGLNDNTIPILARAIIEVGV-----
Ecoli-ASAT  -GRVNVAGMTPDNMAPLCEAIVAVL------
Tb-mASAT    -GRAAVSGLNSTNVEYVSQAIHNVTK-----
Ecoli-ARAT  -GRMCVAGLNTANVQRVAKAFAAVM------
```

**Figure 1.** Structure-based sequence alignment of selected TATs, ASATs, and ARATs. The sequences of the mammalian TATs from *Rattus norvergicus* (rat-TAT, P04694) and *Homo sapiens* (Hum-TAT, P17735); TAT from *Trypanosoma cruzi* (Tc-TAT, P33447); ASATs from *E. coli* (Ecoli-ASAT, P00509) and *Trypanosoma brucei* (mitochondrial [Tb-mASAT, AAK73816]); ARATs from *P. denitrificans* (Pd-ARAT, P95468) and *E. coli* ARAT (Ecoli-ARAT, P04693) are shown for comparison. In the *T. cruzi* sequence, Arg389, Asn17, Arg20, and the equivalent residues in the aligned sequences, as well as Arg292 in the ASATs and ARATs, and Arg417 in mammalian TATs are indicated in bold cases. Deleted amino acids in the rat TAT sequence are denoted in small letters.

Table 1. In contrast to previous findings, implicating the presence of at least three S—S bonds in the rat enzyme (Dietrich et al. 1991), our results clearly show that all 16 cysteine residues per subunit are reduced.

N-terminal sequencing of the recombinant rat enzyme showed the initial methionine to be missing and confirmed the expected sequence for the first 18 amino acids including the six histidine residues corresponding to the His-tag (Table 1).

**Table 1.** *Cysteine containing peptides identified by Edman degradation*

| |
|---|
| 1 EEVASYYHCHEAPLEAK |
| 2 DVILTSGCSQAIELCLAV |
| 3 KTACLVVNNPSNPCGSVFSK |
| 4 QCVPILADEIYGDMVFSDCKY |
| 5 YEPLANLSTNVPILSCGGLAKLSQRILGPCTIVQGALAK |
| 7 SNADLCYGALAAIPGLR |
| 8 LIAEQAVHCLPATCFEYPNFF |
| 9 VVITVPEVMMLEACSR |
| 10 IQEFCEQHYHCAEGSQEECDK |
| $(H)_6$ KARWDVRPSDMS |

The recombinant rat TAT was modified with 4-vinylpyridine, and the tryptic peptides were chromatographed on a Vydac $C_8$ column following the experimental conditions described by Nowicki et al. (2001). The shaded sequence corresponds to that obtained for the N-terminus recombinant rat TAT by Edman degradation.

As previously demonstrated for the full-length rat TAT (Lorber et al. 1991), the truncated enzyme remained intact even after prolonged incubation with trypsin and the intensity of the 45 kD TAT protein band remained constant over this period (data not shown). Thus, the 37 deleted amino acids at the N-terminus have no effect on the conformational properties of the truncated rat TAT.

Spectral studies show that in the pH range from 7 to 8, ionization of the aldimine nitrogen of the rat TAT PLP Schiff base is reflected by pH-dependent changes in the region of 300–500 nm. Similar changes are not observed in *T. cruzi* TAT, reflecting major differences in the p*Ka* values of the internal aldimines of *T. cruzi* and mammalian TATs (Fig. 2A). Unfortunately, the insolubility of both enzymes below pH 6.5 impaired the determination of their internal aldimine pKa values. The absorption band with a maximum at 330 nm represents the nonprotonated PLP form of both TATs, and the peak in the region of 430 nm corresponds to the protonated form. In the mammalian enzyme, the 330 nm absorption maximum shifts, at pH 7.0, to the region of 430 nm due to an increase in the protonated PLP form (Fig. 2A). Addition of L-tyrosine or L-glutamic acid produces an increase in the molar absorptivity at 328 nm, which corresponds to the PMP form (Fig. 2B). Substrate derivatives such as L-α-methyltyrosine, L-α-methylglutamate and *p*-hydroxyphenylpropionate increased the absorption in the region of 430 nm, thus indicating the formation of the corresponding aldimine with PLP, and the competitive aromatic inhibitor complex (Fig. 2C).

### *Comparative mutagenesis studies between* T. cruzi *and rat liver TATs*

Mutagenesis was conducted to address the functionality of (1) Arg315, which in the structure-based sequence alignment is shown to be situated, in mammalian TATs, in a position adjacent to the conserved Arg292 in ASATs and ARATs; (2) Arg417, which is conserved in all known aminotransferases and has been demonstrated to be responsible for interacting with the substrate α-carboxylate group; and (3) the putative *T. cruzi* TAT active site residues Asn17 and Arg20 (Blankenfeldt et al. 1999) and its counterparts Asn54 and Arg57 in rat TAT, which are strictly conserved in TATs but differ among all known ASATs (Fig. 1). All mutations were confirmed by complete gene sequencing.

The substitution of Arg417 for Gln yielded a highly expressed but completely inactive enzyme. Figure 3A shows that the Arg417Gln variant exhibits an intense absorption peak around 430 nm, which does not shift to the region of 330 nm in the presence of tyrosine or glutamate, as it would be expected upon generation of the corresponding PMP form.

Three different rat TAT Arg315 variants were constructed. The Arg315Glu and Arg315Gln substitutions led mainly to the expression of the enzymes into inclusion bodies, and the low amounts expressed in the soluble fraction were not stable enough for being characterized. The Arg315Lys variant, in contrast, was expressed at the same levels as the wild-type enzyme, presented identical absorption spectra (data not shown), and exhibited the same specific activity as the wild-type rat TAT (333 $U \cdot mg^{-1}$) towards the substrate pair tyrosine/2-oxoglutarate. In good agreement with these results, the kinetic constants of the Arg315Lys variant remained unchanged in comparison with those of the wild-type enzyme (Table 2). In contrast, in the ASATs and ARATs the Arg292Lys substitution detrimentally affected the $k_{cat}$ and $K_m$ values of both enzymes (Vacca et al. 1997; Okamoto et al. 1998).

The *T. cruzi* Asn17Ser and Arg20Ala/Gln mutants possess nearly 20- and 100-fold lower specific activities, respectively, when compared with the parasite wild-type enzyme. Similarly, the specific activity of the rat TAT Asn54Ser variant was nearly 14-fold lower than the value obtained for the mammalian wild-type enzyme, while that of the rat TAT Arg57Ala and Arg57Gln variants were reduced nearly $4 \times 10^4$-fold. Table 2 shows that the Asn54Ser substitution produced nearly a 10-fold increase in the $K_m$ value for 2-oxoglutarate, with the $K_m$ values for tyrosine and glutamate also increasing. Furthermore, the $k_{cat}$ values were significantly lower for all the substrates assayed, with the $k_{cat}/K_m$ ratios for tyrosine, glutamate, and 2-oxoglutarate decreasing 11-, 120-, and 43-fold, respectively (Table 2).

The overall kinetic constants could not be determined for the rat TAT Arg57Ala/Gln mutants, due to their low activities and the lack of saturation kinetics with respect to the substrate concentration. Additionally, the Arg57Ala variant showed a higher molar absorptivity than the wild-type enzyme, at pH 7, in the region of 430 nm (Fig. 3A). The Arg57 mutants show identical spectral changes on addition of tyrosine or aromatic substrate analogs, such as *p*-hydroxy-

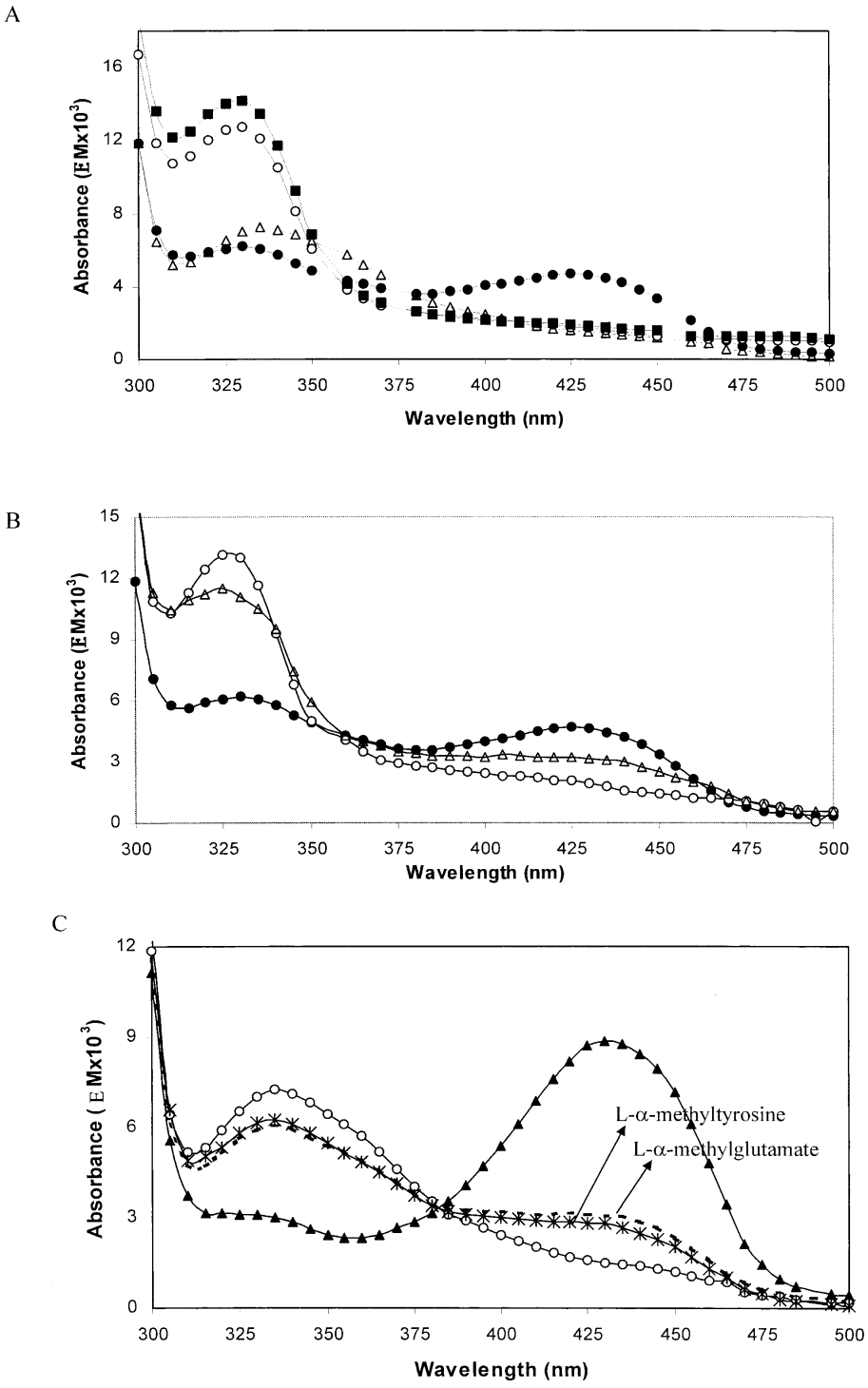


**Figure 2.** Absorption spectra of rat and *T. cruzi* TATs. The spectra were recorded, at 25°C, in 150 mM HEPES-NaOH buffer, 1 mM EDTA, 1 mM DTT, 0.1 M KCl, pH 7.0, and 150 mM Tris-HCl buffer, 1 mM EDTA, 1 mM DTT, 0.1 M KCl, pH 8.0. (*A*) Rat TAT holoenzyme at pH 7.0 (filled circles) and pH 8.0 (open triangles); *T. cruzi* TAT holoenzyme at pH 7.0 (open circles) and pH 8.0 (filled squares). (*B*) Rat TAT holoenzyme at pH 7.0 (filled circles); in the presence of 5 mM tyrosine (open circles), and 60 mM glutamate (open triangles). (*C*) Rat TAT holoenzyme at pH 8.0 (open circles); in the presence of: 20 mM *p*-hydroxyphenylpropionate (filled triangles), 12.5 mM L-α-methyltyrosine (**x**), 20 mM L-α-methylglutamate (- - -).

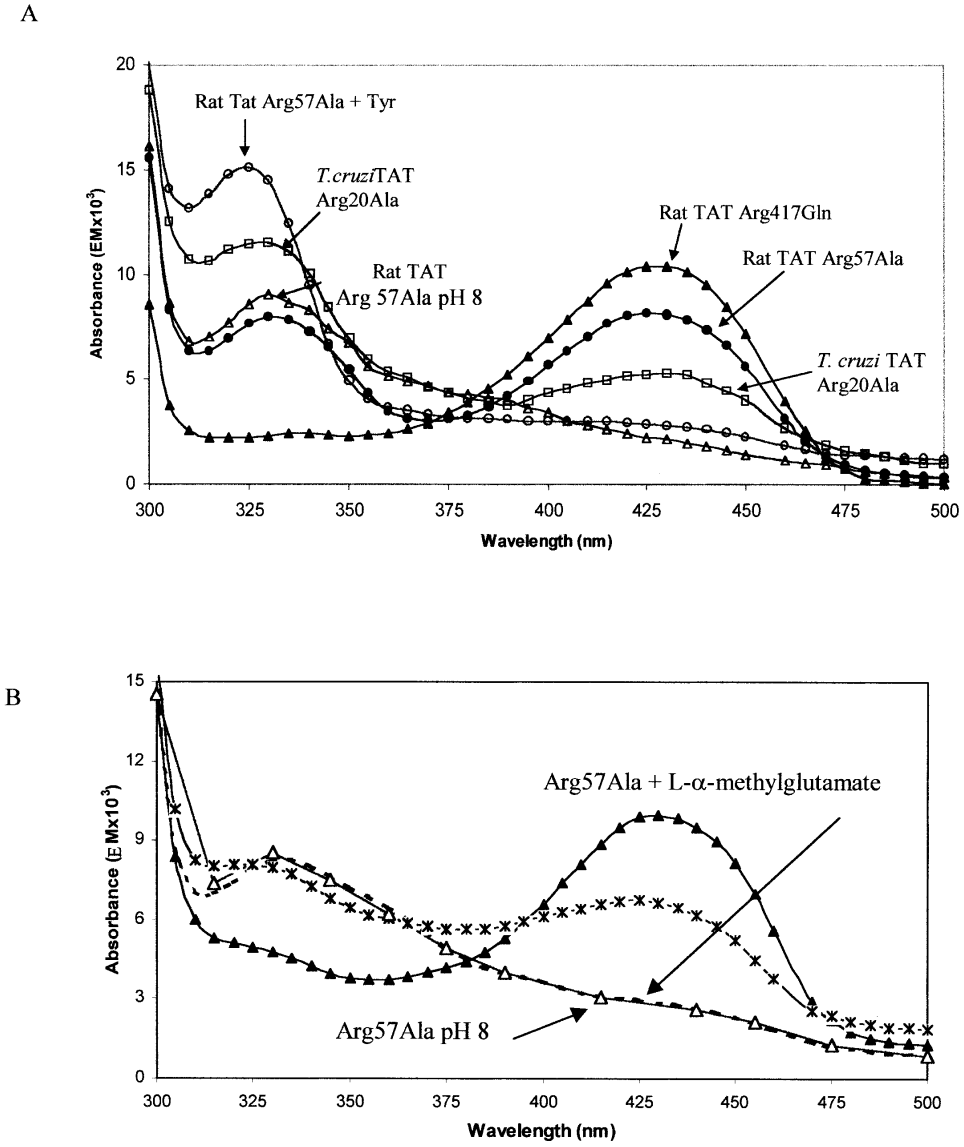


**Figure 3.** (Continued on next page)

phenylpropionate and L-α-methyltyrosine (Fig. 3A,B), and exhibit the same molar absorptivities as the wild-type enzyme in the presence of 5 mM tyrosine (Figs. 2B, 3A). The spectra of both mutants did not alter on the addition of L-α-methylglutamate (Fig. 3B), indicating that, in contrast to the wild-type enzyme, the protonated aldimine was not formed in the presence of this substrate derivative under our experimental conditions. The present results indicate that the Arg57 variants are able to catalyze the first half-reaction using their aromatic substrate L-tyrosine. However, the second half-reaction is significantly slower, with the PLP form being regenerated on the scale of minutes (Fig. 3C). Similarly, the Arg57Ala TAT PLP form is converted to the PMP form at notably slow rates upon the addition of glutamate (Fig. 3D). Evaluation of the dissociation constants ($K_d$) of the Arg57 variants and wild-type enzyme for L-tyrosine, L-glutamate, and *p*-hydroxyphenylpropionate demonstrates unaltered affinities for aromatic substrates but a decrease in affinity for the dicarboxylic acid upon mutation of Arg57 (Table 3). The unchanged dissociation constants for the aromatic substrates imply that the loss of enzymatic activity on substitution of Arg57 is not due to unspecific conformational changes.

The Asn17Ser mutation, in the *T. cruzi* TAT, did not significantly affect the $K_m$ values of the mutant but the $k_{cat}$ values were lowered for all the substrates assayed. The highest decrease in $k_{cat}/K_m$ ratio (47-fold) was observed for tyrosine as substrate (Table 4).

The exchange of Arg20 for Ala in *T. cruzi* TAT produced a similar effect in the absorption pattern in the region of 430

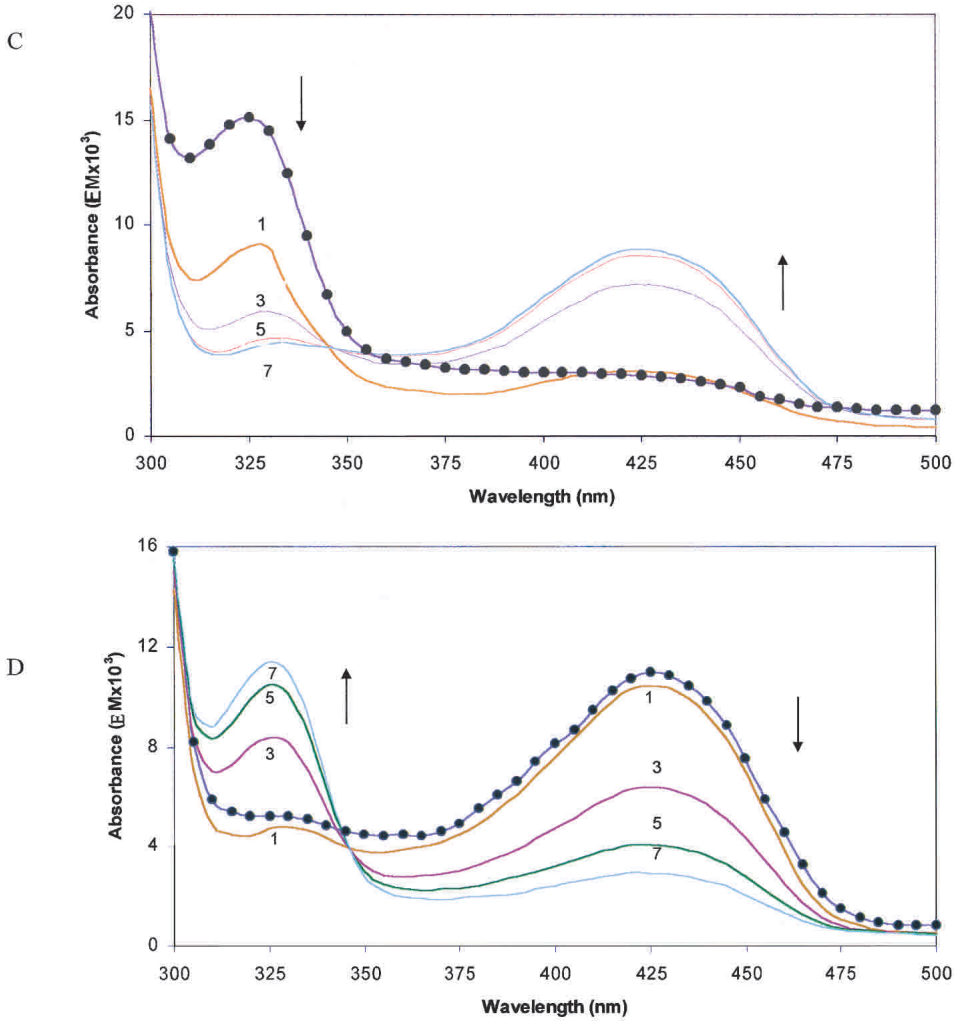


**Figure 3.** Absorption spectra of rat TAT Arg57Ala and Arg417Gln variants, and *T. cruzi* TAT Arg20Ala mutant. The spectra were recorded, at 25°C, in 150 mM HEPES–NaOH buffer, 1 mM EDTA, 1 mM DTT, 0.1 M KCl, pH 7.0, and 150 mM Tris-HCl buffer, 1 mM EDTA, 1 mM DTT, 0.1 M KCl, pH 8.0. (*A*) Rat TAT Arg57Ala at pH 7.0 (filled circles); rat TAT Arg57Ala at pH 8.0 (open triangles); rat TAT Arg57Ala at pH 7.0 in the presence of 5 mM tyrosine (open circles); *T. cruzi* TAT Arg20Ala mutant at pH 7 (open squares); rat TAT Arg417Gln at pH 7.0 (filled triangles). (*B*) Rat TAT Arg57Ala holoenzyme pH 8.0 (open triangles); in the presence of: 20 mM *p*-hydroxyphenylpropionate (filled triangles), 12.5 mM L-α-methyltyrosine (**x**), 20 mM L-α-methylglutamate (- - -). (*C*) Time dependence of the rat TAT Arg57Ala PMP form reaction with 2-oxoglutarate. Spectra were recorded for the first 7 min of incubation of the mutated enzyme with 5 mM 2-oxoglutarate at pH 7.0. Rat TAT Arg57Ala PMP form before (filled circles) and 1 min (1), 3 min (3), 5 min (5), and 7 min (7) after addition of 2-oxoglutarate. The arrows indicate increases and decreases in absorbance. (*D*) Time dependence of the rat TAT Arg57Ala PLP reaction with glutamate. Spectra were recorded for the first 7 min of incubation of the mutated enzyme with 50 mM L-α-glutamate at pH 7.0, before (filled circles) and 1 min (1), 3 min (3), 5 min (5), and 7 min (7) after addition of glutamate. The arrows indicate increases and decreases in absorbance.

nm to that observed with the rat TAT Arg57Ala mutant (Fig. 3A), although the specific activity was less drastically affected. This substitution seems not to alter significantly the $K_m$ values towards the substrates listed in Table 4, although the most affected appears to be 2-oxoglutarate. However, all of the corresponding $k_{cat}$ values decreased and the $k_{cat}/K_m$ ratios for tyrosine, alanine, 2-oxoglutarate, and 2-oxoisocaproate were reduced 124-, 87-, 157-, and 85-fold, respectively (Table 4).

## Discussion

The expression conditions established for rat TAT yielded high quantities of a soluble recombinant truncated enzyme enabling its rapid and simple purification. This recombinant TAT, although shortened by the first 37 amino acids compared to the naturally expressed enzyme in liver cells, remained resistant to trypsin treatment and exhibited identical $K_m$ and $k_{cat}$ values to those of the full-length rat TAT

**Table 2.** *Kinetic parameters for the overall reactions of the N-truncated recombinant rat TAT, Arg315Lys, and Asn54Ser variants*

| Kinetic parameters | Substrate pair | Wild type | Arg315Lys | Asn54Ser |
|---|---|---|---|---|
| $K_m$ (mM) | L-Tyrosine | 2.1 ± 0.3 | 2.3 ± 0.3 | 5.3 ± 0.8 |
| | 2-oxoglutarate | 0.40 ± 0.04 | 0.35 ± 0.05 | 3.5 ± 0.5 |
| $k_{cat}$ ($sec^{-1}$) | L-Tyrosine | 576 ± 50 | 510 ± 43 | 132 ± 15 |
| | 2-oxoglutarate | 566 ± 30 | 490 ± 60 | 116 ± 27 |
| $k_{cat}/K_m$ ($sec^{-1} \cdot M^{-1} \cdot 10^3$) | L-Tyrosine | 274 ± 46 (100) | 222 ± 34 (81) | 25 ± 5 (9) |
| | 2-oxoglutarate | 1415 ± 160 (100) | 1400 ± 263 (99) | 33 ± 9 (2) |
| $K_m$ (mM) | L-Glutamate | 2.2 ± 0.4 | 1.9 ± 0.5 | 8.8 ± 0.8 |
| | *p*-hydroxyphenylpyr | 1.2 ± 0.2 | 1.2 ± 0.3 | 1.3 ± 0.3 |
| $k_{cat}$ ($sec^{-1}$) | L-Glutamate | 210 ± 35 | 199 ± 20 | 6.6 ± 0.4 |
| | *p*-hydroxyphenylpyr | 165 ± 30 | 155 ± 30 | 5.9 ± 0.7 |
| $k_{cat}/K_m$ ($sec^{-1} \cdot M^{-1} \cdot 10^3$) | L-Glutamate | 96 ± 23 (100) | 105 ± 29 (109) | 0.80 ± 0.08 (0.8) |
| | *p*-hydroxyphenylpyr | 138 ± 34 (100) | 129 ± 41 (93) | 4.5 ± 1.2 (3) |

The values, which are the means of at least three experiments, correspond to the steady-state kinetic parameters determined following the experimental conditions described by Nowicki et al. (2001). The concentration ranges of the tested amino acids are indicated in Materials and Methods. The percentage of the relative $k_{cat}/K_m$ values are shown in parentheses.

(Dietrich et al. 1991; Lorber et al. 1991). Peptide sequence analysis demonstrated that in the rat TAT, similarly to the *T. cruzi* enzyme, and in contrast to previous observations (Dietrich et al. 1991), all the cysteines are in the reduced form. The relatively high abundance of cysteine residues in the rat and *T. cruzi* aromatic aminotransferases is in good agreement with the higher sequence similarity observed between the *T. cruzi* and mammalian liver TATs (70%) than between TATs and ASATs (25%; Nowicki et al. 2001).

*T. cruzi* and rat TATs show differences in their spectra in the 300–500-nm region, which reflect a higher pKa value of the rat TAT Schiff base (Fig. 2A). The higher molar absorptivity of the *T. cruzi* TAT around 330 nm (Fig. 2A), as well as the absence of an absorption peak in the region of 430 nm, in the presence of its substrate derivatives, in contrast to rat TAT, ASATs, and ARATs, may be a consequence of a lower pKa value of the Schiff base of the parasite enzyme (Fig. 2C; Hayashi et al. 1967; Nowicki et al. 2001). However, quantitative measurement of the pKa values of the internal aldimines of the N-terminally truncated rat TAT and the His-tagged recombinant *T. cruzi* TAT was impaired by their low solubility below pH 6.5.

ASATs and ARATs display two absorption peaks, at 360 and 430 nm, for their nonprotonated and protonated PLP forms, respectively, and a maximum at 330 nm for their PMP form (Hayashi et al. 1993). In contrast, mammalian and *T. cruzi* TATs possess a maximum at 330 nm corresponding to the nonprotonated internal aldimine, which is nearly the same as that of the C4′ saturated derivative of pyridoxal phosphate, the PMP form. Similarly, other PLP-dependent enzymes, such as rat liver alanine aminotransferase, aspartate aminotransferase from *Sulfolobus solfataricus* and *Treponema denticola* cystalysin, also display an absorption maximum at 330 nm for their nonprotonated PLP form (Matsuzawa and Segal 1968; Marino et al. 1988; Bertoldi et al. 2002). The absorbing species at 430 nm were unequivocally attributed to a protonated aldimne. However, in the latter enzymes, the molecular features responsible for the absorption peak at 330 nm that possess the non protonated PLP, are still not understood.

**Table 3.** *Dissociation constants* ($K_d$) *for wild-type, Arg 57Ala, and Arg57Gln variants of N-truncated rat TAT*

| Rat TAT | *p*-OH-phenylpropionate $K_d$ (mM) | L-glutamate $K_d$ (mM) | L-Tyrosine $K_d$ (mM) |
|---|---|---|---|
| Wild type | 0.9 ± 0.1 | 1.5 ± 0.2 | 1.2 ± 0.1 |
| Arg57Ala | 1.2 ± 0.2 | 5.4 ± 0.7 | 1.3 ± 0.1 |
| Arg57Gln | 1.1 ± 0.2 | 5.9 ± 0.3 | 1.1 ± 0.9 |

The values, which are the means of at least three determinations, were obtained as described in Materials and Methods.

The highly specific rat TAT, like the less specific bacterial ARATs, efficiently utilizes substrates containing a β-carboxylate group, such as 2-oxoglutarate and glutamate, as well as nonpolar aromatic substrates, such as tyrosine. Structure-based sequence alignment shows the rat TAT to contain an arginine at position 315 (Fig. 1), adjacent to *Escherichia coli* Arg292 and conserved in mammalian TATs, which could take on the same role as Arg292 does in *Paracoccus denitrificans* ARAT, moving into the active site to neutralize the substrate β-carboxylate group and outwards for the recognition of the aromatic substrates (Okamoto et al. 1998). However, the guanidine group of Arg315 has been shown to be nonessential for the rat TAT functionality, because the kinetic constants of the Arg315Lys variant are identical to those of the wild-type enzyme. In contrast, the substitution of Arg292 for Lys in *E. coli* ASAT had a large influence on both the $k_{cat}$ and $K_m$ values (Vacca et al. 1997); and in *E. coli* ARAT it had a major effect on the $K_m$ values towards the aromatic and dicarboxylic substrates (Hayashi et al. 1996). Thus, rat TAT seems to be more

**Table 4.** *Kinetic parameters for the overall reactions of the recombinant* T. cruzi *TAT, Asn17Ser, and Arg20Ala variants*

| Kinetic parameters | Substrate pair | Wild type | Asn17Ser | Arg20Ala |
|---|---|---|---|---|
| $K_m$ (mM) | L-Tyrosine | 1.20 ± 0.08 | 2.4 ± 0.4 | 2.3 ± 0.5 |
| | Pyruvate | 0.80 ± 0.07 | 0.60 ± 0.08 | 0.6 ± 0.1 |
| $k_{cat}$ ($sec^{-1}$) | L-Tyrosine | 44.6 ± 1.9 | 1.8 ± 0.3 | 0.70 ± 0.08 |
| | Pyruvate | 47.4 ± 5.2 | 1.50 ± 0.07 | 0.50 ± 0.07 |
| $k_{cat}/K_m$ ($sec^{-1} \cdot M^{-1} \cdot 10^3$) | L-Tyrosine | 37.2 ± 2.9 (100) | 0.8 ± 0.2 (2) | 0.30 ± 0.07 (0.8) |
| | Pyruvate | 59.2 ± 8.3 (100) | 2.5 ± 0.3 (4) | 0.8 ± 0.2 (1) |
| $K_m$ (mM) | L-Alanine | 0.9 ± 0.1 | 1.2 ± 0.2 | 1.2 ± 0.1 |
| | 2-oxoglutarate | 4.6 ± 0.4 | 9.6 ± 1.3 | 14.8 ± 2.1 |
| $k_{cat}$ ($sec^{-1}$) | L-Alanine | 23.5 ± 3 | 3.8 ± 0.3 | 0.35 ± 0.03 |
| | 2-oxoglutarate | 21.8 ± 4 | 4.2 ± 0.6 | 0.50 ± 0.05 |
| $k_{cat}/K_m$ ($sec^{-1} \cdot M^{-1} \cdot 10^3$) | L-Alanine | 26.1 ± 4.4 (100) | 3.2 ± 0.6 (12) | 0.3 ± 0.03 (1) |
| | 2-oxoglutarate | 4.7 ± 1 (100) | 0.4 ± 0.1 (9) | 0.030 ± 0.006 (0.6) |
| $K_m$ (mM) | L-Alanine | 1.1 ± 0.2 | 1.3 ± 0.1 | 1.2 ± 0.2 |
| | 2-oxoisocaproate | 0.60 ± 0.05 | 0.30 ± 0.05 | 0.7 ± 0.1 |
| $k_{cat}$ ($sec^{-1}$) | L-Alanine | 21.2 ± 2.2 | 3.2 ± 0.4 | 0.40 ± 0.07 |
| | 2-oxoisocaproate | 20.4 ± 2 | 2.8 ± 0.2 | 0.30 ± 0.04 |
| $k_{cat}/K_m$ ($sec^{-1} \cdot M^{-1} \cdot 10^3$) | L-Alanine | 19.3 ± 4 (100) | 2.5 ± 0.4 (13) | 0.30 ± 0.06 (2) |
| | 2-oxoisocaproate | 34 ± 4 (100) | 9.3 ± 1.7 (30) | 0.40 ± 0.08 (1) |

The values, which are the means of at least three experiments, correspond to the steady-state kinetic parameters determined following the experimental conditions described by Nowicki et al. (2001). The concentration ranges of the tested amino acids are indicated in Materials and Methods. The percentage of the relative $k_{cat}/K_m$ values are shown in parentheses.

closely related to *T. cruzi* TAT than to the subfamily Iα aminotransferases, as the *T. cruzi* enzyme has also no essential arginine in the region of Arg 292 in *E. coli* ARATs (Nowicki et al. 2001). In contrast, as expected from the sequence alignment, Arg417 of rat TAT seems to play the same role as Arg386 in all ASATs and ARATs.

Based on the *T. cruzi* TAT 3D structure, two residues, Asn17 and Arg20 in *T. cruzi* TAT, and Asn54 and Arg57 in rat TAT, were identified as potential partners for substrate interaction in these enzymes. In good agreement with this hypothesis, substitutions of the corresponding residues in *T. cruzi* and rat TATs significantly lowered the specific activities of the mutants towards their substrates. The exchange of Arg57 for Ala or Gln in rat TAT diminished the overall enzymatic activity nearly $4 \times 10^4$-fold. The absorbance spectra of the Arg57Ala and Arg57Gln mutants as well as their dissociation constants for tyrosine and *p*-hydroxyphenylpropionate demonstrate that the Arg57 substitution does not affect the enzyme′s affinity for aromatic substrates. The higher dissociation constants determined for both variants towards glutamate indicate a decrease in the affinity for the dicarboxylic substrate. Additionally, the slow formation of the PMP form in the presence of glutamate and the slow regeneration of the PLP enzyme on addition of 2-oxoglutarate implies that the rates of both reactions are affected. Thus, the rat Arg57 mutants appear to be catalytically competent despite their extremely low activity. The increased absorption at 430 nm of the mammalian Arg57Ala and *T. cruzi* Arg20Ala TAT variants, at pH 7, implies that they possess a higher Schiff base pKa value than the wild-type enzymes. This electrostatic effect due to the substitution of the Arg residue to Ala suggests that a positive charge was eliminated from the active site of these enzymes without causing gross conformational changes, and resembles the effect observed when Arg292 was exchanged for neutral residues in ARATs and ASATs and when Lys109 was similarly substituted in *T. thermophilus* ASAT (Nobe et al. 1998; Mizuguchi et al. 2001). Thus, Arg57 in rat TAT seems to be functionally equivalent to Arg292 of subfamily Iα aminotransferases for the recognition of dicarboxylic substrates. Substitution of the analogous Arg20 for Ala or Gln does not have such a dramatic effect on *T. cruzi* TAT activity. This mutation significantly decreases the $k_{cat}$ values but has no significant effect on the $K_m$ values for any of the substrates, except for 2-oxoglutarate. As a result, mutation of Arg20 significantly decreases the catalytic efficiency, $k_{cat}/K_m$, of the parasite enzyme (Table 4).

In the *Thermus thermophilus* ASAT only the N-terminal region (Lys13-Val30) of the small domain approaches the active site upon maleate binding instead of the substrate induced large movement of the whole small domain observed on active site closure in the ASATs of the subfamily Iα (Nakai et al. 1999). Arg292 is not conserved in *T. thermophilus* ASAT; however, Lys109, Thr17 and Trp140 have been shown to interact with the substrate's β-carboxylate group (Nakai et al. 1999). From the 3D structure of *T. cruzi* TAT, it seems plausible that the N-terminal α-helix may also play the role of a lid that encloses the substrates in the active site pocket by a similar mechanism to that described for *T. thermophilus* ASAT, with Arg20 and Asn17 taking on the role of Lys109 and Thr17. Unfortunately, structures of the *T. cruzi* TAT in complex with a suitable substrate have

not been resolved to date. However, modeling based on the opened form of its 3D structure shows that only a small movement of the N-terminal arm would be necessary for Asn17 to form a hydrogen bond to the side chain of a tyrosine modeled in a position corresponding to experimental substrate complexes of ASATs (Fig. 4).

In Figure 4 we compare the experimentally determined binding modes of cytosolic pig ASAT complexed with L-α-methylglutamate (1AJS), and *T. thermophilus* ASAT with L-aspartate (1BKG) with the modeled mammalian TAT showing the bifurcated hydrogen bonds that might be expected to connect both carboxylate groups of L-glutamate with the guanidino groups of Arg57 and Arg417. The unchanged $K_m$ values for the *T. cruzi* TAT asparagine and arginine mutants can be rationalized assuming that substrate binding is dominated by the salt bridge formation between the substrate's α-carboxylate group and the strictly conserved arginine residue in the position of Arg386 in ASATs. The herein mutated asparagine and arginine residues may induce the proper substrate orientation by hydrogen bonding in concurrence with active site closure. On the basis of the *T. cruzi* TAT 3D structure, Arg20 is expected to play a similar role to Arg292 of ASATs, as its side chain points away from the active center in the unligated structure, and it would require to be reoriented concomitantly with a movement of the N-terminal α-helix upon substrate binding. In aromatic aminotransferases, it was clearly demonstrated that several nonpolar residues in the N-terminal region are required for the efficient binding of aromatic substrates (Malashkevich et al. 1995a; Onuffer and Kirsch 1995; Shaffer et al. 2002). Presently, it cannot be ruled out that besides Asn17 and Arg20 additional residues of the N-terminal region participate in the catalytic process of *T. cruzi* TAT and/or facilitate substrate-induced domain movement. It may be possible that the significant decreases in the $k_{cat}$ values of these mutants could reflect a slowdown of active site closure, which would result in a detrimental effect on the catalytic efficiency.

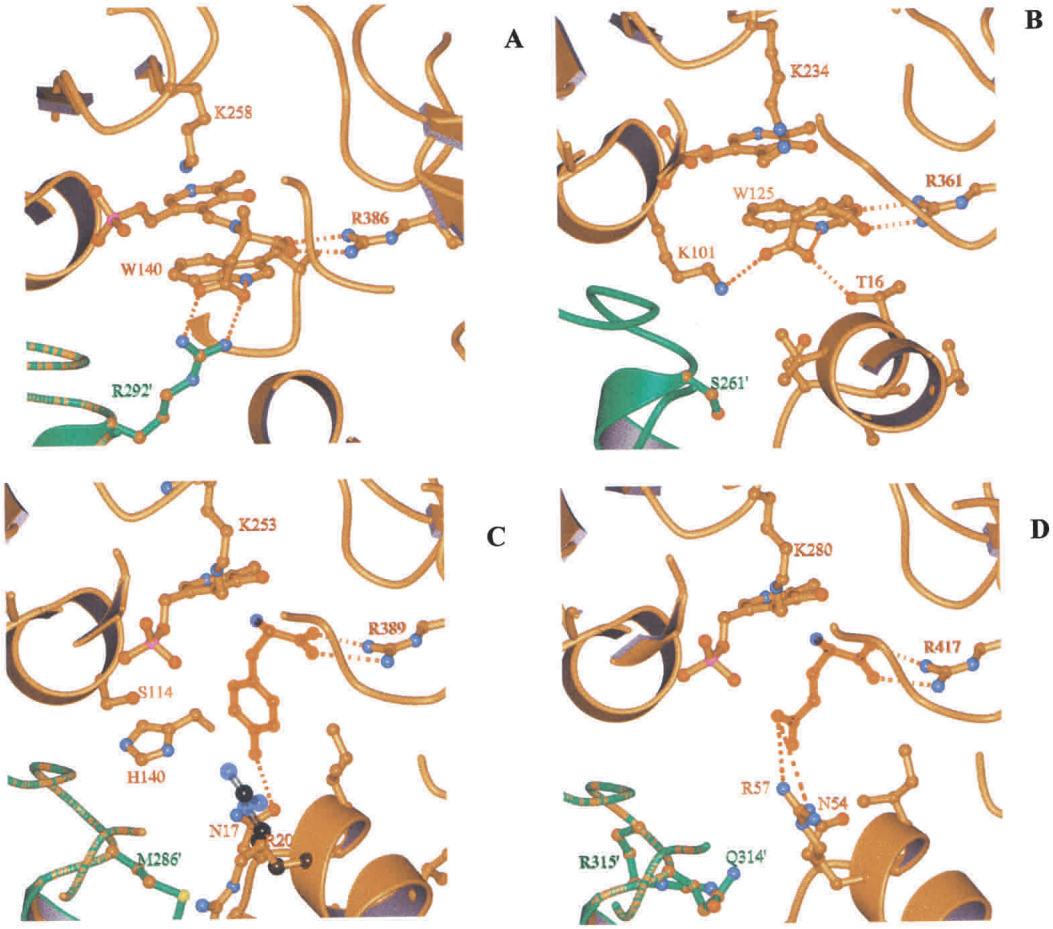


**Figure 4.** Comparison of the active sites of aminotransferases with different substrates specificities. (*A*) Cytosolic pig ASAT complexed with L-α-methylglutamate (1AJS), (*B*) *T. thermophilus* ASAT with L-aspartate (1BKG), (*C*) *T. cruzi* TAT (1BW0) with L-tyrosine modeled as substrate, and (*D*) mammalian TAT model with L-glutamate in the active site. (Prepared with Molscript [Kraulis 1991] and rendered with POV-Ray, www.povray.org.)

The results presented in this work support the hypothesis of Jensen and Gu (1996) that phylogenetically, the mammalian TATs are more closely related to the aromatic aminotransferases from primitive unicellular eukaryotes, such as *T. cruzi,* than to the mammalian ASATs or bacterial ARATs. *T. cruzi* TAT may probably represent a contemporary ancestor for more specialized catalysts such as the mammalian TATs. Further structural and biochemical studies will help to provide a better understanding of the catalytic mechanism of the parasite and mammalian TATs. In this respect, new approaches are currently under way in our laboratory.

## Materials and methods

### *Gene and sequence*

The sequences of *T. cruzi* and rat liver TATs were established earlier (accession number L00673 and NM_012668, respectively). *T. cruzi* TAT was cloned as described previously (Nowicki et al. 2001). A DNA fragment encoding the rat TAT enzyme shortened by the first 37 amino acids but containing six histidines at the N-terminus was amplified by PCR. For the amplification reaction, we used as template a pUC8 recombinant plasmid carrying the full-length cDNA encoding the full-length rat TAT gene, Deep Vent DNA polymerase, and gene-specific oligonucleotides flanking the 5′and 3′ gene ends. The forward primer contained a NdeI restriction site (5′ aaa cat atg cac cac cac cac cac cac aag gcc aga tgg gac gtc aga cc 3′) and the reverse primer contained a XhoI restriction site (5′ ttc aag ctt ctc gag ttt gtc aca ctc ctc ctg gct gcc 3′). The amplified fragment was cloned in a pET24a(+) vector and sequenced by a 373 automatic DNA sequencer (Applied Biosystems), using specific primers for the TAT gene and the PRISM Ready Reaction Dye Deoxy Terminator Sequencing kit.

### *Site-directed mutagenesis of* T. cruzi *and rat liver TAT genes*

A site-directed mutagenesis system (Stratagene) was used to mutate selected codons in the *T. cruzi* and rat liver TAT cloned genes. Complementary oligonucleotides (35–45 mers) containing the appropriate base alterations (in bold) were synthesized according to the corresponding gene sequences: (1) *T. cruzi* TAT: (a) Arg20Ala mutant: fw 5′ ctc gtg ttc aac ccc att **gct** acc gtt tcg gac aac, 3′ rv 5′ gtt gtc cga aac ggt **agc** aat ggg gtt gaa cac gag 3′; (b) Arg20Gln mutant: fw 5′ ctc gtg ttc aac ccc att **cag** act gtt tcg gac aac gcc 3′; rv 5′ ggc gtt gtc cga aac agt **ctg** aat ggg gtt gaa cac gag 3′; (c) Asn17Ser mutant: fw 5′ cat gcc gga ctc gtg ttc **tca** ccc att cgc acc gtt tcg 3′; rv 5′ cga aac ggt gcg aat ggg **tga** gaa cac gag tcc ggc atg 3′; (2) Rat liver TAT: (a) Arg315Lys mutant: fw 5′ ggg ctg gtc aaa ctg agt cag **aaa** atc ctg gga cca tgc 3′; rv 5′ gca tgg tcc cag gat **ttt** ctg act cac ttt cac cag ccc 3′; (b) Arg315Glu mutant: fw 5′ ggg ctg gtc aaa ctg agt cag **gaa** atc ctg gga cca tgc 3′; rv 5′ gca tgg tcc cag gat **ttc** ctg act cac ttt cac cag ccc 3′; (c) Arg315Gln mutant: fw 5′ ggg ctg gtc aaa ctg agt cag **cag** atc ctg gga cca tgc 3′; rv 5′ gca tgg tcc cag gat **ctg** ctg act cac ttt cac cag ccc 3′; (d) Asn54Ser mutant: fw5′ gac atg tcc aat aag acc ttc **tcc** ccc atc cgc gcc atc g 3′, rv 5′ c gat ggc gcg gat ggg **gga** gaa ggt ctt att gga cat gtc 3′; (e) Arg57Ala mutant: fw 5′ cc aat aag acc ttc aat ccc ata **gcc** gcc atc gtg gac aac atg 3′, rv 5′ cat gtt gtc cac gat ggc **ggc** tat ggg att gaa ggt ctt att gg 3′ (f) Arg57Gln mutant: fw 5′ cc aat aag acc ttc aat ccc ata **caa** gcc atc gtg gac aac atg 3′, rv 5′ cat gtt gtc cac gat ggc **ttg** tat ggg att gaa ggt ctt att gg 3′; (g) Arg417Gln mutant: fw 5′ c cca aat ttc ttc caa gtg gtc atc aca gtc c 3′, rv 5′ g gac tgt gat gac cac ttg gaa gaa att tgg g 3′.

### *Soluble expression and purification of recombinant and variant* T. cruzi *and rat liver TATs*

The purified recombinant and mutated plasmids were used to transform *E. coli* BL21(DE3) codon plus strain. Bacterial cultures (1 L) were grown to an $A_{600}$ of 0.6–0.9 in LB medium containing 30 μg/mL kanamycin and 30 μg/mL tetracycline. Expression of the *T. cruzi* TAT was induced overnight at a final concentration of 0.1 mM isopropyl-β-D-thiogalactopyranoside (IPTG), at 28°C. Rat liver TAT expression was carried out under the same experimental conditions with the exception that a final concentration of 0.05 mM IPTG was used and cells were collected after 4-h induction.

Wild-type and mutated enzymes were purified by $Ni^{2+}$-nitrilotriacetic acid resin chromatography according to the supplier's instructions (Qiagen). The purity of the enzyme preparations was assessed by SDS-PAGE. All mutants were expressed at similar levels relative to the respective wild-type enzymes and were electrophoretically homogeneous on purification (data not shown).

### *Determination of TAT activity*

TAT activity was assayed during purification by the method of Diamondstone (1966) without the addition of diethylthiocarbamate and following the experimental conditions previously described (Montemartini et al. 1993). For the mammalian TAT, the assay mixture contained 150 mM triethanolamine buffer, pH 7.5, 1 mM DTT, 1 mM EDTA, 9 mM 2-oxoglutarate, and 5 mM L-tyrosine in a final volume of 1 mL; for the *T. cruzi* enzyme identical conditions were used except that 2-oxoglutarate was replaced by 10 mM pyruvate. The reactions were started by the addition of the corresponding enzymes.

For kinetic studies *T. cruzi* and rat liver TAT activities were determined spectrophotometrically, at 37°C, and at 340 nm in 1-mL reaction mixtures using 150 mM triethanolamine buffer, pH 7.5 (Nowicki et al. 2001). The final concentration ranges for the tested amino acids were: 1–6 mM L-tyrosine, 1–30 mM L-alanine, and 1–50 mM L-glutamate; and for the tested 2-oxoacids were: 1–50 mM pyruvate, 0.5–60 mM 2-oxoglutarate, 0.5–35 mM 2-oxoisocaproate, and 0.5–5 mM *p*-hydroxyphenylpyruvate. All kinetic constants were determined with a computer program fitting the data to a hyperbola by applying the Gauss-Newton algorithm (Fraser and Suzuki 1973).

### *Protein characterization*

Protein concentration was determined according to the method of Bradford (1976) using bovine serum albumin as standard.

Absorption spectra of the wild-type and mutated recombinant rat liver TAT were recorded with a UV/Vis Ultrospec 4000 spectrophotometer (Amersham Biosciences) using 150 mM Tris-HCl buffer, pH 8.0, and 150 mM HEPES, pH 7.0, containing 1 mM EDTA and 1 mM DTT.

The $K_d$ values for L-tyrosine, and L-glutamate were determined, at pH 7.0, by spectrophotometric titration and after 20 min incubation at room temperature. For *p*-hydroxyphenylpropionate the $K_d$ value was obtained, at pH 8.0. The absorbance changes were monitored at 328 nm for L-tyrosine and L-glutamate, and at 430 nm for *p*- hydroxyphenylpropionate. Data were fitted to theoretical curves (Kallen et al. 1985).

Rat TAT in its pyridoxamine 5′-phosphate (PMP) form was obtained as previously described except that tyrosine was used as an amino donor (Hayashi et al. 1993).

Limited proteolysis was performed following the procedure previously described (Lorber et al. 1991).

The presence of disulfide bonds was investigated in rat TAT by chemical modification with 4-vinylpyridine, tryptic digestion, and amino acid sequence analysis of the purified peptides as previously described (Nowicki et al. 2001).

## Acknowledgments

We are grateful to Dr. Thiery Grange for providing us with the full-length rat TAT cDNA and Dr. Hugo Adamo for critical reading of the manuscript. This work was performed with grants from Volkswagen Stiftung, Hannover, Germany, WTZ, BMBF, Bonn, Germany, CONICET, Ministry of Health (Carrillo-Oñativia Fellowship), and Agencia Nacional de Promoción Científica y Tecnológica (Argentina). C.N. is a member of the Research Career from the National Research Council of Argentina (CONICET), V.R.S. is a student fellow of Buenos Aires University, and M.C. delaF. is supported by Carrillo-Oñativia grant from the Ministry of Health (Argentina).

The publication costs of this article were defrayed in part by payment of page charges. This article must therefore be hereby marked "advertisement" in accordance with 18 USC section 1734 solely to indicate this fact.

## References

Alexander, F.M., Sandmeier, E., Mehta, P.K., and Christen, P. 1994. Evolutionary relationships among pyridoxal-5′-phosphate-dependent enzymes. Regio-specific α, β and γ families. *Eur. J. Biochem.* **219:** 953–960.

Arnone, A., Rogers, P.H., Hyde, C.C., Briley, P.D., Metzler, C.M., and Metzler, D.E. 1985. Crystallographic studies of pig and chicken cytosolic aspartate aminotransferase. In *Transaminases* (eds. P. Christen and D.E. Metzler), pp. 138–154. John Wiley and Sons, New York.

Bertoldi, M., Cellini, B., Clausen, T., and Voltattoni, B. 2002. Spectroscopic and kinetic analyses reveal the pyridoxal 5′-phosphate binding mode and the catalitic features of the *Treponema denticola* cystalysin. *Biochemistry* **41:** 9153–9164.

Blankenfeldt, W., Nowicki, C., Montemartini-Kalisz, M., Kalisz, H.M., and Hecht, H.J. 1999. Crystal structure of *Trypanosoma cruzi* tyrosine aminotransferase: Substrate specificity influenced by cofactor binding. *Protein Sci.* **8:** 2406–2417.

Bradford, M.M. 1976. A rapid quantitative method for the quantitation of microgram quantities of protein utilizing the principle of protein-dye binding. *Anal. Biochem.* **72:** 248–54.

Diamondstone, T.I. 1966. Assay of tyrosine transaminase activity by conversion of p-hydroxyphenylpyruvate to p-hydroxybenzaldehyde *Anal. Biochem.* **16:** 395–401.

Dietrich, J.B, Lorber, B., and Kern, D. 1991. Expression of mammalian tyrosine aminotransferase in *Saccharomyces cerevisiae* and *Escherichia coli*. Purification to homogeneity and characterization of the enzyme overproduced in the bacteria. *Eur. J. Biochem.* **201:** 399–407.

Ford, C.G., Eichele, G., and Jansonius, J.N. 1980. Three-dimensional structure of a pyridoxal phosphate dependant enzyme, aspartate aminotransferase. *Proc. Natl. Acad. Sci.* **7:** 2559–2563.

Fraser, R.D.B. and Suzuki, E. 1973. The use of least squares in the data analysis. In *Physical principles and techniques of protein chemistry* (ed. S.J. Leach), part C, vol. 21, pp. 301–355. Academic Press, New York.

Hayashi, H. 1995. Pyridoxal enzymes: Mechanistic diversity and uniformity. *J. Biochem.* **118:** 463–473.

Hayashi, H., Granner, D., and Tomkins, G. 1967. Tyrosine aminotransferase. Purification and characterization. *J. Biol. Chem.* **242:** 3998–4006.

Hayashi, H., Inoue, K., Nagata, T., Kuramitsu, S., and Kagamiyama, H. 1993. *Escherichia coli* aromatic amino acid aminotransferase: Characterization and comparison with aspartate aminotransferase. *Biochemistry* **32:** 12229–12239.

Hayashi, H., Inoue, H., Mizuguchi, H., and Kagamiyama, H. 1996. Analysis of the substrate-recognition mode of aromatic amino acid aminotransferase by combined use of quasisubstrates and site-directed mutagenesis: Systematic hydroxy-group addition/deletion studies to probe the enzyme-substrate interactions. *Biochemistry* **35:** 6754–6761.

Iwasaki, Y., Lamar, C., Danenberg, K., and Pitot, C. 1973. Studies on the induction and repression of enzymes in rat liver. Characterization and metabolic regulation of multiple forms of tyrosine aminotransferase. *Eur. J. Biochem.* **34:** 347–357.

Jensen, R.A. and Gu, W. 1996. Evolutionary recruitment of biochemically specialized subdivisions of family I within the protein superfamily of aminotransferases. *J. Bacteriol.* **178:** 2161–2171.

Kallen, R.G., Korpela, T., Martell, A.E., Matsushima, Y., Metzler, C.M., Metzler, D.E., Morozow, Y.V., Ralston, I.M., Savin, F.A., Torchinsky, Y.M., et al. 1985. Chemical and spectroscopic properties of pyridoxal and pyridoxamine phosphate. In *Transaminases* (eds. P. Christen and D.E. Metzler), pp. 37–108. John Wiley and Sons, New York.

Kirsch, J.F., Eichele, G., Ford, G.C, Vincent, G.M., Jansonius, J.N., Gehring, H., and Christen, P. 1984. Mechanism of action of aspartate aminotransferase proposed on the basis of its spatial structure. *J. Mol. Biol.* **174:** 497–525.

Kraulis, P.J. 1991. Molscript: A program to produce both detailed and schematic plots of protein structures. *J. Appl. Crystallogr.* **24:** 946–950.

Lorber, B., Dietrich, J.B., and Kern, D. 1991. Isolation and characterization of active N-terminal truncated apo- and holoenzymes of mammalian liver tyrosine aminotransferase. *FEBS Lett.* **291:** 345–349.

Malashkevich, V.N., Onuffer, J.J., Kirsch, J.F., and Jansonius, J.N. 1995a. Alternating arginine-modulated substrate specificity in an engineered tyrosine aminotransferase. *Nat. Struct. Biol.* **2:** 548–553.

Malashkevich, V.N., Strokopitov, B.V., Borisov, V.V., Dauter, Z., Wilson, K.S, and Torchinsky, Y.M. 1995b. Crystal structure of the closed form of chicken cytosolic aspartate aminotransferase at 1.9 Å resolution. *J. Mol. Biol.* **247:** 111–124.

Marino, G., Nitti, G., Arnone, M.I., Sannia, G., Gambacorta, A., and De Rosa, M. 1988. Purification and characterization of aspartate aminotransferase from the thermophilic archaebacterium *Sulfolobus solfataricus*. *J. Biol. Chem.* **263:** 12305–12309.

Matsuzawa, T. and Segal, H. 1968. Rat liver alanine aminotransfrase. Crystallization, composition, and role of the sulfhydryl groups. *J. Biol. Chem.* **243:** 5929–5934.

McPhalen, C.A, Vincent, M.G., Picot, D., Jansonius, J.N., Lesk, A.M., and Chothia, C. 1992. Domain closure in mitochondrial aspartate aminotransferase *J. Mol. Biol.* **227:** 197–213.

Mizuguchi, H., Hayashi, H., Okada, K., Miyahara, I., Hirotsu, K., and Kagamiyama, H. 2001. Strain is more important than electrostatic interaction in controlling the pKa of the catalytic group in aspartate aminotransferase. *Biochemistry* **40:** 353–360.

Montemartini, M., Santomé, J.A., Cazzulo, J.J., and Nowicki, C. 1993. Purification and partial structure and kinetic characterization of tyrosine aminotransferase from *Trypanosoma cruzi*. *Biochem. J.* **292:** 901–906.

Nakai, T., Okada, K., Akutsu, S., Miyahara, I., Kawaguchi, S., and Kato, R. 1999. Structure of *Thermus thermophilus* HB8 aspartate aminotransferse and its complex with maleate. *Biochemistry* **38:** 2413–2424.

Nobe, Y., Kawaguchi, S., Ura, H., Nakai, I., Hirotsu, K., Kab, R., and Kuramitsu, S. 1998. The novel substrate recognition mechanism utilized by aspartate aminotransferase of the extreme thermophile *Thermus thermophilus* HB8. *J. Biol. Chem.* **273:** 29554–29564.

Nowicki, C., Reynoso Hunter, G., Montemartini-Kalisz, M., Blankenfeldt, W., Hecht, H.J, and Kalisz, H.M. 2001. Recombinant tyrosine aminotransferase from *Trypanosoma cruzi*: Structural characterization and site directed mutagenesis of a broad substrate specificity enzyme. *Biochim. Biophys. Acta* **1546:** 268–281.

Okamoto, A., Nakai, Y., Hayashi, H., Hirotsu, K., and Kagamiyama, H. 1998. Crystal structures of *Paracoccus denitrificans* aromatic amino acid aminotransferase: A substrate recognition site constructed by rearrangement of hydrogen bonds network. *J. Mol. Biol.* **280:** 443–461.

Onuffer, J.J. and Kirsh, J.F. 1995. Redesigned of the substrate specificity of *Escherichia coli* aspartate aminotransferase to that of *Escherichia coli* tyrosine aminotransferase by homology modelling and site directed mutagenesis. *Protein Sci.* **4:** 1750–1757.

Oue, S., Okamoto, A., Nakai, Y., Nakahira, M., Shibatani, T., Hayashi, H., and Kagamiyma, H. 1997 *Paracoccus denitirficans* aromatic amino acid aminotransferase: A model enzyme for the study of dual substrate recognition mechanism. *J. Biochem.* **121:** 161–171.

Shäffer, W.A., Luong, T.N., Rothman, S.C., and Kirsch, J.F. 2002. Quantitative chimeric analysis of six specificity determinants that differentiates *Escherichia coli* aspartate from tyrosine aminotransferase. *Protein Sci.* **11:** 2848–2859.

Stellwagen, R.H. 1992. Involvement of sequences near both amino and carboxyl termini in the rapid intracellular degradation of tyrosine aminotransferase. *J. Biol. Chem.* **267:** 23713–23721.

Vacca, R.A, Giannatassio, S., Graber, R., Sandmeier, E., Marra, E., and Christen, P. 1997. Active-site Arg → Lys substitutions alter reaction and substrate specificity of aspartate aminotransferase. *J. Biol. Chem.* **272:** 21932–21937.